Modelling and short-term forecasting of seasonal mortality

Ainhoa-Elena Leger[a], Silvia Rizzi[a], Ugofilippo Basellini[b]

[a]*Interdisciplinary Centre on Population Dynamics (Cpop), Odense,*
[b]*Max Planck Institute for Demographic Research (MPIDR), Rostock,*

Abstract

Excess mortality, i.e., the difference between expected and observed mortality, is used to quantify the death toll of mortality shocks, such as epidemics and pandemics of infectious diseases. However, predictions of expected mortality are sensitive to model assumptions. We analyse which specification of a Poisson regression for seasonal mortality yields more accurate predictions. We compare the Poisson Serfling model with 1) parametric effect for the trend and seasonality, 2) non-parametric effect for the trend and parametric effect for the seasonality, and 3) non-parametric effect for the trend and seasonality, also known as modulation model. Forecasting is achieved with P-splines smoothing. Model 2) resulted in more accurate historical forecasts on the series of monthly deaths from national statistical offices in 25 European countries. An application to the COVID-19 pandemic years illustrates how excess death can be used to evaluate the vulnerability of populations and aid public health planning.

Keywords: excess mortality, baseline estimation, P-splines, smoothing, seasonality

1. Introduction

Measuring the mortality burden related to natural and health shocks provides fundamental information to aid public health responses by guiding policy-making decisions. It offers insights into the vulnerability of populations, the geographical gradient, and the effect of the policies adopted in response to the shock. Excess mortality is a useful indicator to assess the impact of influenza outbreaks (Mazick et al., 2012; Mølbak et al., 2015; Nielsen et al., 2018), heat waves (Fouillet et al., 2006; Toulemon and Barbieri, 2008) and pandemics of infectious diseases, such as the 1918–1920 H1N1 influenza pandemic (Ansart et al., 2009) and the 2019 coronavirus pandemic (Kontis et al., 2020; Islam et al., 2021).

Excess death is computed as the difference between the expected deaths and the reported deaths in the same period. The expected deaths (or baseline mortality) are predicted in a counterfactual scenario where no mortality shock had happened. The mortality difference, ceteris paribus, can be considered as overall effect of the mortality shock. The predictions of the expected deaths are usually obtained in the short term, i.e., within an epidemic year to study the effect of the influenza season, or over a few years in the case of several waves of new pandemics of infectious diseases.

The methodological choices about how to forecast mortality are crucial, since different models lead to varying estimates of excess death. Various models were proposed for estimating the expected deaths, which show considerable seasonal variation, mostly striking harder in winter than in summer in Europe. The first attempt to model a "standard curve of expected seasonal mortality" accounting for long-time trends and seasonal variation goes back to the contribution of Serfling (1963). This method is based on a linear regression that models the deaths during an epidemiological year as a linear function of time (long-time trend) and one or more sinusoidal terms (seasonal variation). More recently employed models are Poisson Serfling regressions (Thompson et al., 2009) considering the count nature of mortality data, and Quasi-Poisson Serfling accounting for over-dispersion (EuroMOMO, 2017).

Although widely used, a limitation of the Poisson Serfling model is the assumption of the linearity of the trend on the logarithmic scale, which can lead to the under or over-estimation of excess mortality if the trend is not linear. Eilers et al. (2008) introduced the modulation models that relax the linearity assumption by considering smooth long-term trends and smooth seasonal effects over time. The models use regression splines, specifically B-splines with penalties, known as P-splines (Eilers and Marx, 1996). The regression with P-splines leads to a generalized linear model, which is fitted by penalized likelihood. Our aim in this study is to extend the modulation models for seasonal mortality forecasting purposes. We do so by following the approach by Currie et al. (2004). The authors describe the approach within the scope of forecasting death rates over extended periods, such as 50 years, or from a cohort perspective. This method integrates P-splines regression with a missing value approach. The same approach can be used for forecasting seasonal mortality in the short term. Future values are considered as missing values and estimated simultaneously with the fitting of the mortality model. By modifying the weights in the penalization, forecasting is a natural consequence of the smoothing process.

In this study, we consider the prediction of the baseline mortality when no mortality shock happens. Our study builds on the works of Eilers et al. (2008) and Currie et al. (2004). The modulation models are used as the basis to forecast baseline mortality in the short term via P-splines with a missing value approach. The P-splines smoothing is adapted to predict the expected mortality during one or more epidemiological year. This yields the baseline mortality that is used in the estimation of excess deaths during influenza outbreaks or mortality shocks. We compare the classical Poisson Serfling model with two versions of the modulation models with 1) smooth long-term trends and fixed seasonality and 2) smooth long-term trends and varying seasonal components. For our application of the models, we retrieved from Eurostat the mortality and population data on 25 European countries.

In Section 2, we describe our proposed forecasting strategy. We start by reviewing the Poisson Serfling model, and then show the two variants of the modulation model, illustrating the estimation and forecasting strategy. In Section 3, we describe our data sets. In Sections 4 and 5, we describe our choices for the models' parameters, respectively for mortality modelling and mortality forecasting. We show an application to the estima-

tion of excess mortality during the COVID-19 pandemic. The paper concludes with a critical discussion of our methodology and the findings for the excess death estimation.

2. Methods

This section first presents the model traditionally used in the literature to predict seasonal mortality (subsection 2.1) and the proposed models with detailed description of the regression matrix and penalty matrix (subsections 2.2 and 2.3). The method for estimating and forecasting with P-splines is then adapted to seasonal data (subsection 2.4 and 2.5). Finally, we explain the measures that will be used to evaluate the goodness of fit of the model and the accuracy of the forecasts (subsection 2.6).

2.1. Poisson Serfling (PS) model

Let Y_t be a non-negative random variable denoting the death counts in a population at the months t, with $t = 1, ..., T$. The realizations of Y_t are the observed number of deaths y_t. We assume that the random variable Y_t follows a Poisson distribution with expected values μ_t.

$$Y_t \sim Poi(\mu_t), \quad \mu_t = E[Y_t]$$

The log link function relates the mean μ_t to the linear predictor $log(\mu_t) = \eta_t$.
The first model that we consider is the Poisson Serfling model (Serfling, 1963), which includes a linear trend and models the seasonality using sine and cosine functions.

$$log(\mu_t) = \beta_0 + \beta_1 t + \beta_3 cos(wt) + \beta_4 sin(wt)$$

where $t = 1, \ldots, T$, $w = 2\pi/p$, and p is the period. Analyses in this paper are performed on monthly death counts and rates, so $p = 12$. Estimation of the regression coefficients $\hat{\beta}$ can be performed with the Iterated Weighted Least Squares (IWLS) for GLM models (McCullagh and Nelder, 1989).
The model allow for exposures e_t, when the objective is to model death rates. The Poisson Serfling (PS) with exposures is

$$log(\mu_t) = log(e_t) + \beta_0 + \beta_1 t + \beta_3 cos(wt) + \beta_4 sin(wt).$$

2.2. Smooth trend and smooth seasonality (PS-STSS) model

Secondly, we propose to use the modulation models developed by Eilers et al. (2008) and extend them to forecast the baseline mortality by adapting the P-splines approach of Currie et al. (2004) to seasonal data. The modulation models introduce a smooth trend function and time-varying coefficients. This gives a very general model for demographic seasonal time series. The structure is the following

$$log(\mu_t) = \upsilon_t + f_t cos(wt) + g_t sin(wt), \tag{1}$$

where υ_t accounts for the smooth trend, f_t and g_t are smooth functions that describe the local amplitudes of the cosine and sine waves, and $w = 2\pi/p$, with p the period (e.g.,

$p = 12$ for monthly data). The smooth trend function and the modulation series f_t and g_t are constructed by approximating B-splines basis. Specifically, $\upsilon_t = \sum_j \alpha_j B_j(t)$, $f_t = \sum_j \beta_j B_j(t)$ and $g_t = \sum_j \gamma_j B_j(t)$, with $\boldsymbol{B} = [b_{tj}] = [B_j(t)]$ B-splines basis, $t = 1, \ldots, T$ the time index, and $j = 1, \ldots, J$ the B-splines index.
By introducing the matrices $\boldsymbol{C} = diag\{cos(wt)\}$ and $\boldsymbol{S} = diag\{sin(wt)\}$, the model in Equation 1 can be written in the matrix-vector notation

$$log(\boldsymbol{\mu}) = \boldsymbol{B\alpha} + \boldsymbol{CB\beta} + \boldsymbol{SB\gamma} = \boldsymbol{\eta}$$

where $\boldsymbol{\upsilon} = \boldsymbol{B\alpha}$, $\boldsymbol{f} = \boldsymbol{B\beta}$, $\boldsymbol{g} = \boldsymbol{B\gamma}$. The linear predictor can then be re-arranged

$$\eta = [\boldsymbol{B}|\boldsymbol{CB}|\boldsymbol{SB}][\boldsymbol{\alpha'}|\boldsymbol{\beta'}|\boldsymbol{\gamma'}] = \breve{\boldsymbol{B}}\boldsymbol{\theta}.^{1} \tag{2}$$

When modelling death rates, the exposures e_t are included and the PS-STSS model becomes

$$log(\mu_t) = log(e_t) + \upsilon_t + f_t cos(wt) + g_t sin(wt),$$

2.3. Smooth trend and fixed seasonality (PS-STFS) model

In addition to employing the Poisson Serfling model and the modulation model, we propose an alternative approach to account for smooth trend component and fixed seasonality (STFS). Specifically, we employ the same structure

$$log(\mu_t) = \upsilon_t + \beta_1 cos(wt) + \beta_2 sin(wt).$$

where υ_t accounts for the smooth trend, and the cosine and sine have constant coefficients β_1 and β_2 over time, and $w = 2\pi/p$. The smooth trend function is constructed by approximating B-splines basis. Specifically, $\upsilon_t = \sum_j \alpha_j B_j(t)$, with $\boldsymbol{B} = [b_{tj}] = [B_j(t)]$ B-splines basis, $t = 1, \ldots, T$ the time index, and $j = 1, \ldots, J$ the B-splines index.
The linear predictor models the trend component with the B-splines matrix $\boldsymbol{B}$ and time varying coefficients $\boldsymbol{\alpha}$, and the seasonal component with the vectors $\boldsymbol{c} = cos(wt)$ and $\boldsymbol{s} = sin(wt)$ and the coefficients β_1 and β_2

$$\boldsymbol{\eta} = [\boldsymbol{B}|\boldsymbol{c'}|\boldsymbol{s'}][\boldsymbol{\alpha'}|\beta_1|\beta_2] = \breve{\boldsymbol{B}}\boldsymbol{\theta}. \tag{3}$$

When modelling death rates, the exposures e_t are included and the PS-STFS model becomes

$$log(\mu_t) = log(e_t) + \upsilon_t + \beta_1 cos(wt) + \beta_2 sin(wt).$$

2.4. Estimation

For both versions of the modulation model, the estimation of the models' parameters is achieved using penalized B-splines or P-splines to force them to vary more smoothly (Eilers and Marx, 1996). The B-spline bases model the series υ, f and g and an

[1] From here onward, $\boldsymbol{B}$ indicates the matrix of B-splines, while $\breve{\boldsymbol{B}}$ indicates the regression matrix.

additional penalty on the B-spline coefficients optimizes their amount of smoothing. We minimize the penalized Poisson deviance defined as

$$d^*(y;\mu) = 2\sum_{t=1}^{T} log(y_t/\mu_t) + \lambda_1 \left\|\boldsymbol{D\alpha}\right\|^2 + \lambda_2 \left\|\boldsymbol{D\beta}\right\|^2 + \lambda_2 \left\|\boldsymbol{D\gamma}\right\|^2$$

where the matrix $\boldsymbol{D} = \Delta^d$ constructs dth order differences of $\boldsymbol{\alpha}$, $\boldsymbol{\beta}$ and $\boldsymbol{\gamma}$. For instance, Δ^1 is a matrix $(J-1) \times J$ of first differences and $\boldsymbol{\Delta^1\alpha}$ is the vector with elements $\boldsymbol{\alpha_{j+1}} - \boldsymbol{\alpha_j}$, for $j = 1, \ldots, J-1$. By repeating this computation on $\boldsymbol{\Delta^1\alpha}$, we arrive at higher differences like $\boldsymbol{\Delta^2\alpha}$, where $\boldsymbol{\Delta^2}$ the $(J-2)\times J$ matrix of second-order differences of a J-vector.

The linear re-expressions 2 and 3 allow all of the parameters associated with each components to be estimated simultaneously as GLMs. Estimation of the coefficients is performed via the penalized version of the Iterated Weighted Least Squares (IWLS)

$$(\breve{\boldsymbol{B}}'\widetilde{\boldsymbol{M}}^{(t)}\breve{\boldsymbol{B}} + \boldsymbol{P})\boldsymbol{\theta}^{(t+1)} = \breve{\boldsymbol{B}}'\widetilde{\boldsymbol{M}}^{(t)}\breve{\boldsymbol{B}}\boldsymbol{\theta}^{(t)} + \breve{\boldsymbol{B}}'(\boldsymbol{y} - \tilde{\boldsymbol{\mu}}), \tag{4}$$

where $\breve{\boldsymbol{B}}$ is the regression matrix, $\widetilde{\boldsymbol{M}} = diag(\boldsymbol{\mu})$ is the matrix of weights, and $\boldsymbol{P} = \Lambda\boldsymbol{D'D}$ is the penalty term. The positive penalty hyper-parameter $\Lambda = diag(\lambda_1, \lambda_2, \lambda_2)$ balance smoothness against fit to the data and allows for different penalty for the trend (λ_1) and modulation functions (λ_2). The penalty matrix can also be constructed to consider differents order of the differences for the trend and modulation functions as $\boldsymbol{P} = blockdiag(\lambda_1\boldsymbol{D_1'D_1}, \lambda_2\boldsymbol{D_2'D_2}, \lambda_2\boldsymbol{D_2'D_2})$. For instance, Carballo et al. (2019) suggests an order of differences of 2 and 1 for λ_1 and λ_2, respectively.

The modulation model presents some similarities with some other models in the literature. The smooth trend component $\boldsymbol{\upsilon}$ can be seen as a generalized additive model (GAM, Hastie and Tibshirani 1990) and the seasonal components $\boldsymbol{f}$ and $\boldsymbol{g}$ as a varying-coefficient model (VCM, Hastie and Tibshirani 1993). The advantage of P-splines over GAM and VCM is that they avoid both the backfitting algorithm and complex knot selection schemes.

2.5. Forecasting with P-splines

Following Currie et al. (2004), the forecasting of future values can be treated as a missing value problem and the fitted and forecast values can be estimated simultaneously. Consider observing the death counts y_1 for n_1 months and wanting to forecast n_2 months into the future. Let us define a new time index t_+ with $t_+ = 1, ..., n_1, ..., n_1+n_2$. To obtain the fit and the forecast simultaneously, we extend for $n_1 + n_2$ months the regression matrix $\breve{\boldsymbol{B}}$ and the penalty matrix $\boldsymbol{P}$. The IWLS algorithm of Equation 4 is adapted as follows:

$$(\breve{\boldsymbol{B}}'_+\boldsymbol{V}\widetilde{\boldsymbol{M}}^{(t)}\breve{\boldsymbol{B}}_+ + \boldsymbol{P}_+)\boldsymbol{\theta}^{(t+1)} = \breve{\boldsymbol{B}}'_+\boldsymbol{V}\widetilde{\boldsymbol{M}}^{(t)}\breve{\boldsymbol{B}}_+\boldsymbol{\theta}^{(t)} + \breve{\boldsymbol{B}}'_+\boldsymbol{V}(\boldsymbol{y} - \tilde{\boldsymbol{\mu}}),$$

where the matrix $\breve{\boldsymbol{B}}_+ = [\breve{\boldsymbol{B}}_+|\boldsymbol{C}_+\boldsymbol{B}_+|\boldsymbol{S}_+\boldsymbol{B}_+]$ is the extended regression matrix and the matrix $\boldsymbol{P}_+ = blockdiag(\lambda_1\boldsymbol{D'_{1+}D_{1+}}, \lambda_2\boldsymbol{D'_{2+}D_{2+}}, \lambda_2\boldsymbol{D'_{2+}D_{2+}})$ is the extended penalty

matrix. It follows that $\breve{\boldsymbol{B}}_+$ is the extended matrix of B-splines for the trend, $\boldsymbol{C}_+ = diag(cos(wt_+))$ and $\boldsymbol{S}_+ = diag(sin(wt_+))$ are the extended matrices for the modulation components, and $\boldsymbol{D_{1+}}$ and $\boldsymbol{D_{2+}}$ are the extended matrices of differences. Furthermore, a matrix $\boldsymbol{V} = blockdiag(\boldsymbol{I}; \boldsymbol{0})$ weights 1 the observations ($\boldsymbol{I}$ has size n_1) and 0 the forecasts ($\boldsymbol{0}$ has size n_2).
The confidence intervals for the fitted values and the prediction intervals (PI) for the forecasts are computed simultaneously using the approximate variance of $\breve{\boldsymbol{B}}_+\hat{\boldsymbol{\theta}}$ given by

$$Var(\breve{\boldsymbol{B}}_+\hat{\theta}) \approx \breve{\boldsymbol{B}}_+(\breve{\boldsymbol{B}}'_+\boldsymbol{V}_+\widetilde{\boldsymbol{M}}\breve{\boldsymbol{B}}_+ + \boldsymbol{P}_+)^{-1}\breve{\boldsymbol{B}}'_+.$$

2.6. Evaluation measures

To evaluate the model performance balancing the goodness of fit and the model complexity, we will use the Bayesian Information Criterion BIC defined as (Schwarz, 1978)

$$\text{BIC} = 2\text{Dev} + \log \text{n Tr}$$

where Dev is the deviance of the model, n is the number of observations, and $Tr = tr(\boldsymbol{H})$ is the effective dimension of the fitted model. The hat matrix is defined as $\boldsymbol{H} = \hat{\boldsymbol{M}}^{1/2}\breve{\boldsymbol{B}}(\breve{\boldsymbol{B}}'\hat{\boldsymbol{M}}\breve{\boldsymbol{B}} + \boldsymbol{P})^{-1}\breve{\boldsymbol{B}}'\hat{\boldsymbol{M}}^{1/2}$ and the trace is $tr(\boldsymbol{H}) = tr[\breve{\boldsymbol{B}}'\hat{\boldsymbol{M}}\breve{\boldsymbol{B}}(\breve{\boldsymbol{B}}'\hat{\boldsymbol{M}}\breve{\boldsymbol{B}} + \boldsymbol{P})^{-1}]$.
To evaluate the forecasting accuracy, we will use the Root Mean Squared Error (RMSE) and the Mean Absolute Percentage Error (MAPE). We consider $y_1, \ldots, y_N$ to fit the model (training set) and $y_{N+1}, \ldots, y_T$ to check the forecasting accuracy (test set). The forecasting error is defined as the difference between the observed values and the forecasts $e_t = y_t - \hat{y}_t$, for $t = N+1, \ldots, T$

$$RMSE = \sqrt{mean(e_t^2)} = \frac{1}{T-N}\sum_{t=N+1}^{T} e_t^2.$$

The percentage error is defined as $p_t = 100e_t/y_t$, for $t = 1, \ldots, T$

$$MAPE = mean(|p_t|) = \frac{1}{T-N}\sum_{t=N+1}^{T} |p_t|.$$

3. Data

We retrieved the series of monthly death counts and population counts from Eurostat[2] for 25 countries (Austria, Bulgaria, Croatia, Czechia, Denmark, Estonia, Finland, France, Germany, Greece, Hungary, Iceland, Ireland, Italy, Lithuania, Luxembourg, Netherlands, Norway, Poland, Portugal, Romania, Slovenia, Spain, Sweden, and Switzerland). We selected the countries for which we could access complete series of monthly data that goes back at least to 1995 and extended through June 2022.

[2] https://ec.europa.eu/eurostat

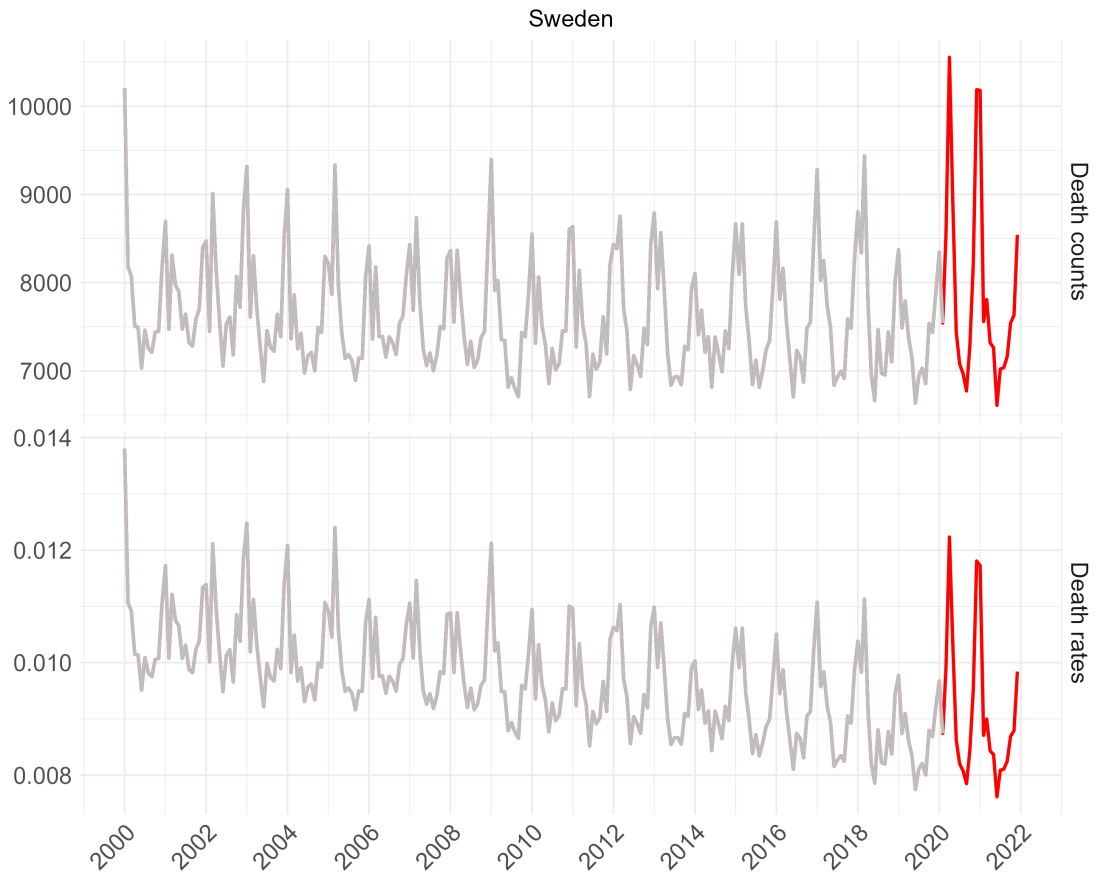

Figure 1: Death counts and death rates from 2010 to 2021 for Sweden. The period before the COVID-19 pandemic is in grey (2009 to February 2020) and the period after the COVID-19 pandemic is in red (March 2020 to 2021).

We use the yearly population counts to obtain the exposures as the mid-point between populations on the 1st January of each year and divided by 12. The deaths and exposure data are arranged respectively in vectors $\boldsymbol{y}$ and $\boldsymbol{e}$ indexed by month. The crude death rates (CDRs) are then computed as $\boldsymbol{y}/\boldsymbol{e}$. CDRs measure the intensity of deaths in a population and are used to project mortality in time and compute a baseline mortality (Aburto et al., 2021; Basellini et al., 2021; Stokes et al., 2021).

Figure 1 shows for illustrative purposes the monthly total death counts and CDRs for Sweden from 2000 to 2021. The series show a strong temporal trend and cyclical behavior, also known as seasonal variation. The CDRs decrease over time, being influenced by improvements in living conditions and mortality. The seasonal variation strikes harder in winter than in summer being driven by seasonal influenza in the older population. The winter peak usually happens every year between December and March. In February 2020, the COVID-19 pandemic struck in Europe disrupting mortality patterns and increasing mortality outside the usual window of December to March. In the two years after the first wave of COVID-19, mortality seems to follow the regular

pattern of seasonal mortality.
Additionally, the series were retrieved disaggregated by sex and age at death from the national statistical offices[3] of the countries that made them available: Denmark (2007 to 2022), Italy (2003 to 2022), Spain (2009 to 2022), and Sweden (2000 to 2022). We grouped the death counts by four age group (0-64, 65-74, 75-84, 85+) because it is the finest age classification available. When comparing mortality across populations, considering the age-specific death rates (ASDRs) instead of the CDRs permits to reduce the influence of the age composition of the population (Németh et al., 2021; Nepomuceno et al., 2022). Age structures can change over time due for instance to population aging (Preston et al., 2001; Djeundje et al., 2022; Missov et al., 2023).

4. The underlying models

The previous section set out the theory for modelling with P-splines. In this section, we explain our choice of the various parameters in the modelling (subsection 4.1), We then compare the performance of the three models (PS, PS-STSS, PS-STFS) in all European countries on the period 1995 to 2019, i.e., in the absence of the mortality schock caused by the COVID-19 pandemic (subsection 4.2).

4.1. Choice of the model's parameters

The parameters to be chosen when fitting the modulation models are 1) the degree of the splines, 2) the number of regions (or equivalently the number of knots) to divide the domain and 3) the penalty hyper-parameters.
The spline's degree controls the order of the polynomial included in the B-spline bases. We used a basis of cubic B-splines (degree 3) for the modulation models. The chosen number of regions to divide the domain is two per year. Therefore, the number of basis depends on the number of years used to predict the baseline. The number of B-splines is the number of divisions plus the degree of the splines. The relation can also be expressed as $nbasis = nknots + bdeg - 1$, with $nbasis$ number of basis functions, $nknots$ number of knots, and $bdeg$ degree of the spline. For instance, let us fit the model on 10 years (from 2010 to 2019): the domain is divided in 20 regions by 21 knots (19 interior knots and 2 knots at the boundaries of the domain) and uses 23 cubic B-splines.
Figure 2 illustrate the non-parametric fit of the trend function v_t with B-splines for Sweden. The results are presented on a logarithmic scale, because the Poisson regression models the logarithm of the expected value. The top panel shows a basis of 23 cubic B-splines. In the middle panel, the B-spline bases locally defined are scaled with the estimated coefficients (e.g. negative coefficients lead to parabulas below zero; the higher the coefficient, the higher the scaled parabula) to fit the monthly death rates

[3]Statistics Denmark, https://www.dst.dk/en, Istituto Nazionale di Statistica https://www.istat.it/, Instituto Nacional de Estadística, https://www.ine.es/en/, Statistics Sweden, https://www.scb.se/en/

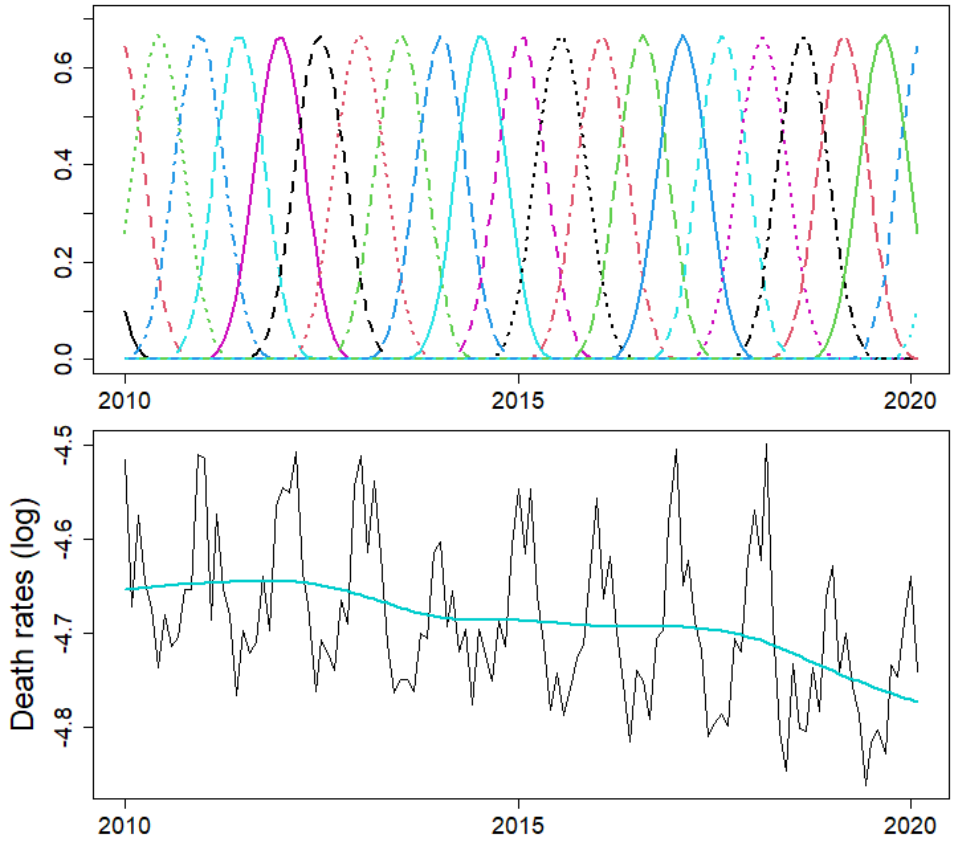

Figure 2: Illustration of the fit (logarithmic scale) of the trend function $\boldsymbol{v} = \boldsymbol{B\alpha}$ with B-splines for Sweden. The panels show: 23 cubic B-spline basis in the top panel, scaled B-spline basis in the middle panel, sum of scaled B-spline basis function in the bottom panel.

(black line). The B-splines slightly widen from 2010 to 2019 to accomodate the decreasing trend in the data. The scaled bases are then summed up to form the smooth trend function v_t that fits the data (light blue line) in the bottom panel. By construction, the B-spline bases are then smoothly joined together.

The P-splines introduce an additional penalty term that prevents overfitting. In the PS-STSS model, the penalty uses second order differences for the trend and first order differences for the seasonal component (Carballo et al., 2019). In the the PS-STFS model, we use second order differences for the trend. The tuning of the penalty hyperparameters λ_1 for the trend and λ_2 for the seasonal component was achieved through MAPE minimization on a grid search. We will explain these choices in detail in subsection 5.1 because they influence the forecasts.

Table 1: Mean BIC on **death rates** in 25 European countries for multiple fitting periods based on a rolling-window scheme.

	5 years series			10 years series		
	PS	PS-STSS	PS-STFS	PS	PS-STSS	PS-STFS
Austria	1032	987	1013	2038	1971	2000
Bulgaria	1895	1836	1847	3809	3671	3722
Croatia	836	800	822	1641	1605	1633
Czechia	1322	1272	1295	2511	2352	2379
Denmark	648	642	653	1346	1305	1327
Estonia	243	252	253	487	488	490
Finland	597	597	608	1214	1203	1218
France	8099	7403	7867	17036	15934	16448
Germany	10556	9582	10099	21869	20058	20837
Greece	2646	2510	2576	5066	4871	4969
Hungary	2163	2056	2124	4143	4046	4090
Iceland	96	108	108	198	214	214
Ireland	686	679	694	1495	1384	1432
Italy	11248	10008	10556	22304	20579	21429
Lithuania	599	586	592	1463	1246	1254
Luxembourg	107	119	119	216	231	231
Netherlands	1853	1773	1813	3753	3596	3616
Norway	618	592	626	1248	1173	1240
Poland	4866	4501	4704	9776	8974	9457
Portugal	3529	3392	3489	6806	6691	6756
Romania	4199	3759	3861	9192	8172	8676
Slovenia	314	315	323	637	640	649
Spain	9435	8614	9026	19226	18056	18568
Sweden	1094	1067	1096	2218	2201	2225
Switzerland	813	783	814	1600	1590	1606
	4	20	1	4	21	0

4.2. Performance of the fitted models

To compare their goodness of fit, the three models (PS, PS-STSS and PS-STFS) were fitted on a rolling window and the model fit was measured with the BIC. We used a 5-years rolling window because it is the standard choice in the literature and 10-years rolling window as a comparison. The three models were fitted on the common period available for the death series, that is from 2010 to 2019. The series' lengths permit the computation of the BIC for a sufficient number of years for both the 5-years rolling window (20 BICs) and the 10-years rolling window (15 BICs). Table 1 shows the mean BIC values obtained by fitting the models on the CDRs. The mean BIC favours the model PS-STSS, which allows for more flexibility of the trend and seasonality, in almost all the countries (20 with 5-years and 21 with 10 years). Either using 5-years or 10-years for the rolling window, the model PS-STSS better fit the series than the PS and the PS-STFS model. The results of fitting the three models to the death counts are showed in the Appendix A (Table A.5) and are similar to the one for the CDRs.

Figure 3 shows the fit of the three models on the CDRs in the logarithmic scale for Sweden (and also show forecasts, which will be discussed later in Section 5). The

trend function $\boldsymbol{v}$ (dashed coloured line) and the fitted values $\hat{\boldsymbol{\mu}}$ (solid coloured line) are overlayed to the observed monthly death counts $\boldsymbol{y}$ (grey line). The results for all the other countries are shown in the Supplementary Materials (Figures 1 to 7).

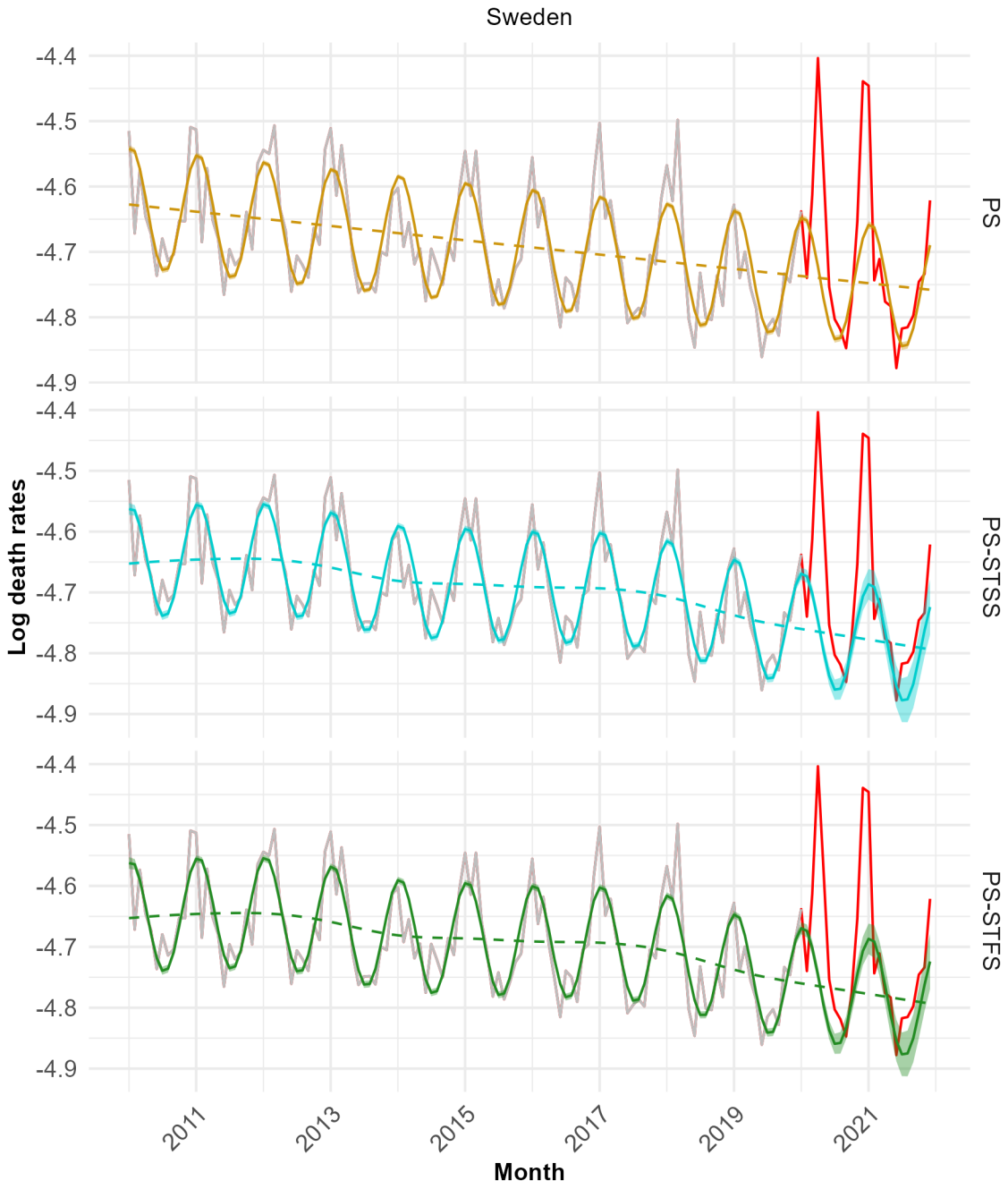

Figure 3: Modelling and forecasting of monthly deaths (logarithmic scale) for Sweden with the Poisson Serfling model (PS) and modulation models (PS-STSS and PS-STFS). Trend function (dashed coloured line), fitted values (solid coloured line).

Sweden has a declining trend of the CDRs according to the three models. However, the trend estimated is linear for the PS model and non linear for the PS-STSS and PS-STFS models with the slope of the regression line changing over time. Furthermore, the PS-STSS and PS-STFS models better fit the mortality level during the summer, especially in the last years of the fitting period before COVID-19. The difference between the model PS-STSS and the model PS-STFS is that they assume respectively a varying seasonality and a fixed seasonality. The fitted models PS-STSS and PS-STFS did not seem to capture a noticeable change in the seasonality.

Our approach is similar to Eilers et al. (2008) because we are not interested in catching the winter spikes. We do not want our model to overfit every year but rather to estimate an average pattern. A small excess deaths can happen every year between December and March due to seasonal influenza occurs. What we are interested in, is the counterfactual forecast and the excess death during a mortality shock, that can happen outside the typical period December-March. Our approach differ from the one in Eilers et al. (2008) that ignores the months from December to March by giving them zero weights. We keep these months in our fitting period because we want to use the information on the location of the winter peak.

The amplitude of the seasonal variation, as described in Eilers et al. (2008), permits further inspection and measurement of the changes of the seasonal component over time. Figure 4 shows the amplitude of the seasonal component obtained with the PS-STSS model in Sweden on the period 2010-2019. The grey line represents the detrended

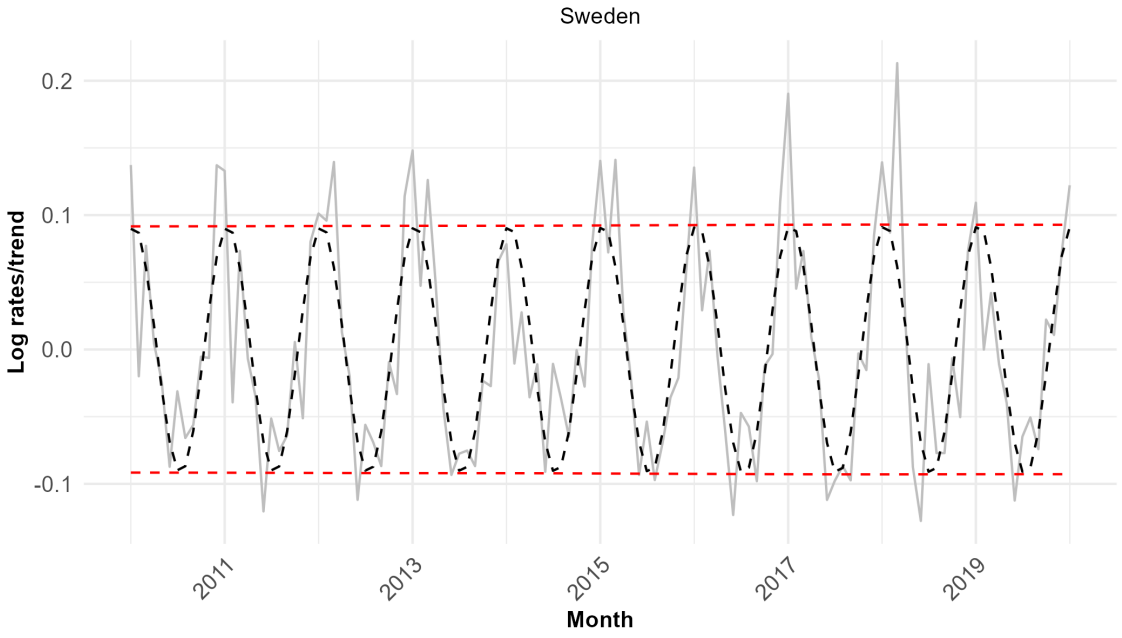

Figure 4: Changes in the seasonal component over time for Sweden, with the modulation models PS-STSS: detrended series (grey), modulated component (dashed black) and amplitude (dashed red).

series, i.e., the ratio $\boldsymbol{y/\hat{\mu}}$, the dashed black line is the modulated component given by $f_t cos(wt) + g_t sin(wt)$, and the red line its amplitude $\boldsymbol{\rho} = \sqrt{(\boldsymbol{f^2 + g^2})}$. The seasonal amplitude remains constant over time in Sweden. Similar results can be observed for the majority of the countries (Supplementary Materials, Figure 8 and 9).

5. Results on the forecasts

The models are applied to obtain out-of-sample predictions of the monthly deaths. First, we explain our choice of the order of the penalty (5.1). We then present forecasting accuracy of the three models (PS, PS-STSS, PS-STFS) on historical periods in the absence of mortality shocks (5.2). Finally, we calculate the excess death during the COVID-19 pandemic (5.3).

5.1. Choice of the order of the penalty

The forecasting method works by extrapolating the regression coefficients and the penalty on the coefficients ensures their smoothness. The order of the penalty determines whether the coefficients are approximately constant (order 1), linear (order 2) or quadratic (order 3). As a consequence, the smoothness of the forecasts also depends on the order of the penalty. Figure 5 shows the effect of changing the order of the penalty on the predictions of the trend. The second order for the trend, i.e., a linear extrapolation, best approximate the mortality trend, while the first order penalty for the modulation functions, gives more realistic predictions and 95% PI.

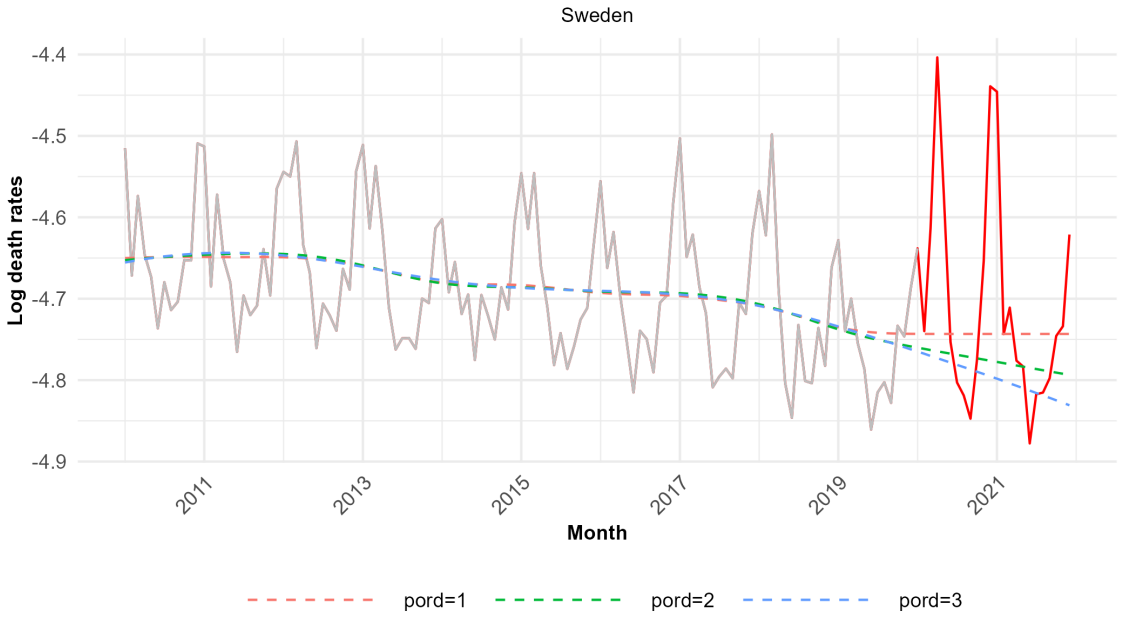

Figure 5: Effect of the order of the penality on the forecasts of the trend function (logarithmic scale), in Sweden, with the model PS-STSS.

Out-of-sample validation was used to chose the order of the penalty that provides better forecasts. We compared the following penalties: first order for the trend and seasonality (T1S1), second order for both the trend and seasonality (T2S2), first order for the trend and second order for the seasonality (T1S2), and second order for the trend and first order for the seasonality (T2S1). The results are shown in Tables B.6 for the death counts and B.7 for the death rates in Appendix B. The model with a second order penalty for the trend and a first order penalty for the seasonality provided a better forecasting accuracy and were then chosen.
The penalty hyper-parameters λ_1 for the trend and λ_2 for the seasonal component were chosen through a rolling window on the estimation set. We used values from 10^4 to 10^7 to compute the predictions one year ahead and chose the hyper-parameters based on the minimum mean MAPE. We decided to use the MAPE minimization instead of the BIC minimization, as the focus of our analysis is on forecasting (rather than modelling). This procedure was applied to both the PS-STSS model and the PS-STFS model.

5.2. Forecasts' evaluation

We evaluated the forecasting accuracy of the three models (PS, PS-STSS and PS-STFS) via out-of-sample validation. A rolling window of 5 years and a rolling window of 10 years were used to predict the deaths counts one year ahead. The accuracy of the forecasts is measured based on the RMSE and MAPE. Like in the case of the BIC comparisons, the series of death counts for the three countries permit to have a sufficient number of years to evaluate the forecasts for both the 5-years rolling window and the 10-years rolling window.
Table 2 shows how well each model could have predicted the rates in the period before the COVID-19 pandemic. When using 5 years as fitting period, the preferred model is the PS for the majority of the countries. However, when using 10 years to fit the models, the forecasting accuracy improves and the PS-STFS model becomes the preferred one. According to the mean MAPE (and mean RMSE), the PS-STFS would have been more accurate in predicting mortality one year ahead in 13 cases out of 25 (and 13 cases for the RMSE) than the PS model (7 and 9 cases) and the PS-STSS model (4 and 3 cases). Therefore, for those countries, the trend is better approximated by more flexible models than a linear interpolation.
Figure 3 plots the model-specific forecasts of the trend function $\boldsymbol{v}$ and the predicted values $\hat{\boldsymbol{\mu}}$ using a second order penalty for the trend and a first order penalty for the modulation functions. The observed monthly death counts $\boldsymbol{y}$ are overlaid in grey on the fitting period (2011 to February 2020) and in red on the forecasting period (February 2020 to June 2022). The forecast of the trend is decreasing according to the three models and the PI are generally wider with the PS-STSS and PS-STFS models than the PS model. The forecast from March 2020 to December 2022 can be considered as the counterfactual mortality had the health shock not occurred. The difference between the forecasts and the observed mortality represents an estimate of the excess mortality attributable to the health shock. Depending on the model, the baseline mortality might differ and lead to different estimations of the excess death.

Table 2: Mean RMSE and MAPE on **death rates** (x 1000) in 25 European countries for multiple fitting periods based on a rolling-window scheme.

	5 years series						10 years series					
	RMSE			MAPE			RMSE			MAPE		
	PS	STSS	STFS	PS	STSS	STFS	PS	STSS	STFS	PS	STSS	STFS
Austria	0.52	0.53	0.53	4.0767	4.1234	4.0596	0.51	0.51	0.50	4.0994	3.9255	3.9046
Bulgaria	0.98	1.01	1.01	4.9998	5.2385	5.1931	0.98	0.96	0.97	4.8537	4.8038	4.8285
Croatia	0.80	0.83	0.82	4.9332	5.1465	5.0552	0.77	0.78	0.78	4.2389	4.4063	4.4265
Czechia	0.56	0.56	0.55	3.8864	3.8202	3.6753	0.54	0.53	0.52	3.7092	3.6305	3.5899
Denmark	0.50	0.51	0.50	3.8477	3.8808	3.8473	0.48	0.48	0.47	3.7556	3.6365	3.5619
Estonia	0.71	0.72	0.72	4.3943	4.4731	4.4573	0.69	0.65	0.65	4.3286	4.1250	4.0721
Finland	0.49	0.50	0.50	3.8159	3.9007	3.9313	0.47	0.47	0.46	3.5913	3.5901	3.5618
France	0.52	0.54	0.53	4.1252	4.4582	4.3770	0.47	0.49	0.47	3.8077	4.0890	3.8456
Germany	0.59	0.61	0.59	3.8427	4.0639	3.9287	0.60	0.59	0.58	3.9127	3.6898	3.6180
Greece	0.76	0.76	0.75	5.3800	5.3538	5.2793	0.74	0.74	0.75	5.1226	5.2597	5.2708
Hungary	0.80	0.83	0.82	4.3044	4.5832	4.4575	0.74	0.74	0.74	3.7969	3.9475	3.9419
Iceland	0.65	0.65	0.65	8.0715	8.0906	8.0861	0.59	0.59	0.59	7.6200	7.5869	7.5903
Ireland	0.49	0.48	0.49	5.3619	5.3767	5.4646	0.46	0.40	0.40	5.4810	4.8639	4.8642
Italy	0.71	0.78	0.77	5.3338	5.8816	5.8434	0.68	0.73	0.72	4.9051	5.3539	5.2955
Lithuania	0.84	0.82	0.81	5.1975	4.9878	4.9635	1.02	0.87	0.87	6.2032	5.2079	5.2212
Luxembourg	0.63	0.64	0.64	6.8401	7.0285	7.0280	0.57	0.57	0.57	6.2410	6.2996	6.2990
Netherlands	0.47	0.48	0.48	3.9835	4.2002	4.1678	0.49	0.46	0.45	4.2544	3.8987	3.8529
Norway	0.52	0.50	0.51	4.8227	4.6813	4.8195	0.49	0.46	0.49	4.9574	4.4858	4.9652
Poland	0.53	0.57	0.55	3.7573	4.0273	3.9733	0.56	0.54	0.54	3.9593	3.7097	3.7087
Portugal	0.84	0.89	0.88	5.7897	6.3081	6.3158	0.82	0.84	0.83	5.5416	5.8212	5.7671
Romania	0.83	0.85	0.85	5.2372	5.3616	5.3515	0.73	0.76	0.78	4.2378	4.6758	4.7223
Slovenia	0.60	0.62	0.61	4.8876	4.9298	4.9272	0.58	0.58	0.58	4.3536	4.3581	4.3155
Spain	0.66	0.69	0.68	5.5342	5.6678	5.5563	0.64	0.62	0.62	5.3792	4.9982	4.9929
Sweden	0.51	0.51	0.50	3.8483	3.8712	3.8042	0.45	0.46	0.45	3.4682	3.5249	3.5009
Switzerland	0.45	0.46	0.46	4.0130	4.1636	4.1387	0.40	0.40	0.40	3.5831	3.5695	3.5038
	17	2	6	18	1	6	7	4	14	9	3	13

In an epidemic year, a significant excess death (i.e., outside the PI) is usually recorded in the months between December and March, when the winter peak occurs. In these months, mortality might exceed the expected deaths with an intensity that depends on the severity of the seasonal influenza. The excess mortality recorded during the COVID-19 pandemic from March 2020 until 2022 is visibly larger than in the previous years. Furthermore, the excess in 2020, corresponding to the first COVID-19 wave, occurred outside the normal epidemic period. After the first wave, the excess death throughout epidemic years 2020/2021 and 2021/2022 reaches a lower peak and follows the seasonal behavior of the influenza deaths.

5.3. Excess death during the COVID-19 pandemic

The number of deaths in excess or deficit were obtained by subtracting the expected deaths, had the COVID-19 pandemic not occurred, to the observed deaths. The expected deaths for the majority of the countries was obtained with the PS-STFS model. We chose the baseline of the PS-STSS model for Ireland, Lithuania, Norway, Poland

Table 3: All-cause excess death in Europe during three pandemic periods (first covid wave, and first and second epidemic year after the shock). Baseline mortality is obtained with the Modulation Models PS-STFS.

country	March to June 2020	July 2020 to June 2021	July 2021 to June 2022
Austria	-172 (-531 ; 183)	8873 (7574 ; 10152)	8154 (6016 ; 10238)
Bulgaria	-1954 (-2237 ; -1673)	34015 (33203 ; 34822)	34863 (33787 ; 35928)
Croatia	-320 (-647 ; 2)	11647 (10333 ; 12927)	13168 (10858 ; 15372)
Czechia	-862 (-1418 ; -313)	35580 (33060 ; 38042)	9453 (4622 ; 14082)
Denmark	-521 (-864 ; -182)	965 (-442 ; 2335)	5655 (3126 ; 8069)
Estonia	-69 (-177 ; 37)	1934 (1627 ; 2236)	2504 (2096 ; 2901)
Finland	158 (-30 ; 344)	325 (-197 ; 842)	6077 (5413 ; 6734)
France	18054 (16906 ; 19196)	58582 (53817 ; 63310)	42477 (33881 ; 50952)
Germany	-2855 (-4399 ; -1318)	69732 (63055 ; 76360)	84476 (72071 ; 96716)
Greece	-2898 (-3511 ; -2292)	4018 (1153 ; 6819)	12820 (7130 ; 18276)
Hungary	-629 (-1178 ; -85)	33175 (30842 ; 35462)	23410 (19193 ; 27483)
Iceland	-37 (-71 ; -4)	-77 (-164 ; 8)	143 (44 ; 239)
Ireland	1013 (828 ; 1196)	944 (350 ; 1527)	2362 (1479 ; 3222)
Italy	43900 (43046 ; 44752)	105750 (102981 ; 108506)	72607 (68461 ; 76726)
Lithuania	588 (374 ; 800)	9971 (9271 ; 10658)	10530 (9482 ; 11548)
Luxembourg	-54 (-101 ; -8)	284 (163 ; 401)	34 (-104 ; 169)
Netherlands	6340 (5983 ; 6696)	10444 (9391 ; 11490)	13677 (12234 ; 15106)
Norway	281 (-77 ; 632)	410 (-769 ; 1555)	3633 (1717 ; 5461)
Poland	-3688 (-4426 ; -2954)	121220 (118979 ; 123449)	60763 (57545 ; 63956)
Portugal	405 (109 ; 699)	15623 (14773 ; 16468)	6241 (5102 ; 7369)
Romania	-1545 (-2161 ; -932)	66455 (64286 ; 68604)	65471 (61995 ; 68901)
Slovenia	-80 (-265 ; 101)	4259 (3578 ; 4918)	2179 (1036 ; 3261)
Spain	42043 (40909 ; 43171)	40576 (35226 ; 45855)	35654 (25204 ; 45842)
Sweden	5582 (5114 ; 6045)	5421 (3374 ; 7418)	5097 (1296 ; 8735)
Switzerland	579 (246 ; 907)	7589 (6344 ; 8812)	4386 (2288 ; 6421)

based on accuracy analysis. Furthermore, the seasonality is correctly modeled for Norway only by the PS-STSS model (Supplementary Materials, Figure 3). We report the number of excess deaths together with their 95% credible intervals in Table 3. The credible intervals represents the uncertainty in how many deaths would have occurred in the absence of the pandemic. Some of the estimates and lower bounds of excess deaths are negative. Negative values imply the saving of lives. For ease of interpretation, we distinguished three phases of the COVID-19 pandemic: 1) the first wave (from March 2020 to June 2020), 2) the epidemic year 2020-21 (from July 2020 to June 2021), and 3) the epidemic year 2021-22 (from July 2021 to June 2022).

Taken all the 25 European countries together, 104,365 (95% credible interval, 92,740–115,897) more people died from February through May 2020 than would have had the pandemic not occurred. Among the European countries, France, Italy, Lituania, Netherlands, Portugal, Spain, Sweden, and Switzerland were hit since the first wave

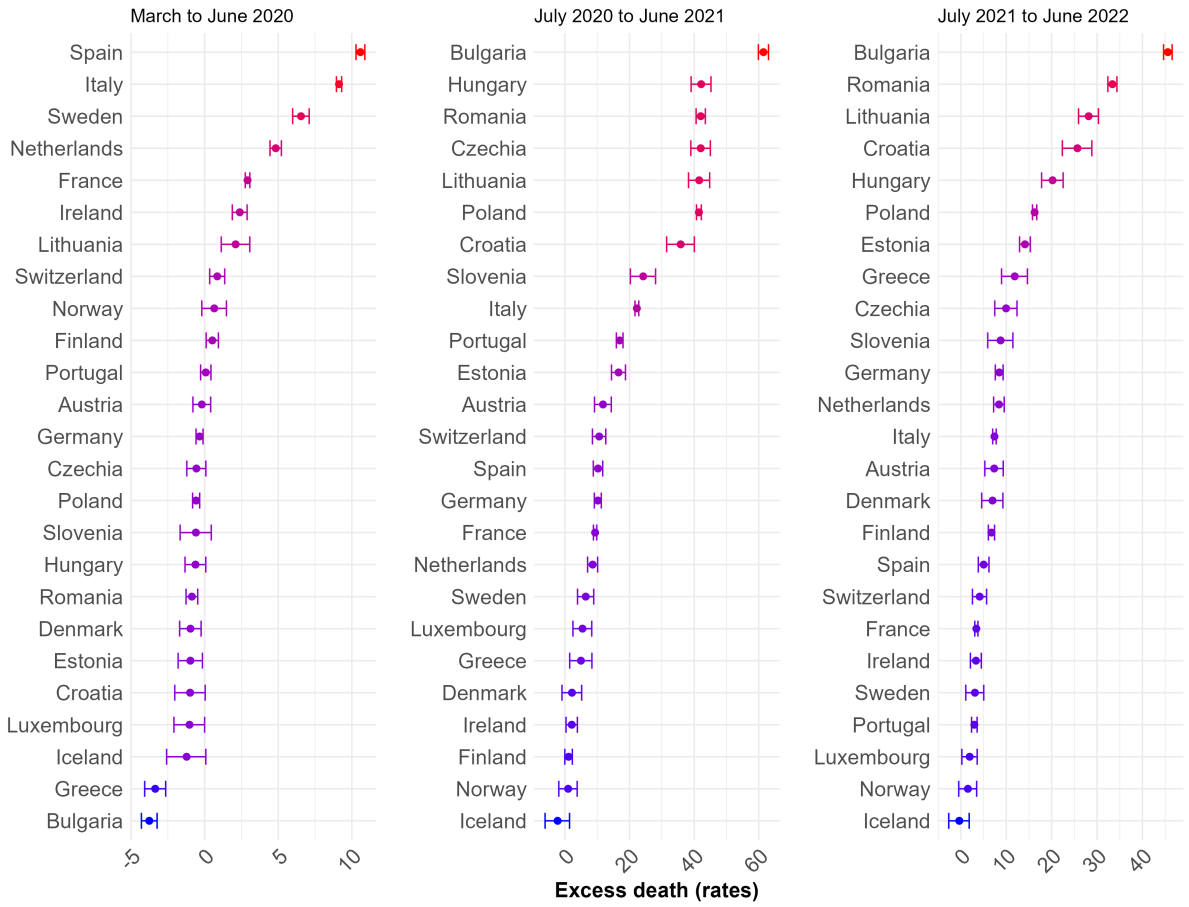

Figure 6: Excess death rates (x 1000) in Europe during three pandemic periods (first covid wave, and first and second epidemic year after the shock). Baseline obtained with the PS-STFS model.

and had excess death in the two following epidemic years, while the remaining countries did not had excess or even avoided deaths in the first wave but were hit later on.

European countries have different sizes and death rates are better suited to compare them. Figure 6 report the excess death rates together with their 95% credible intervals. During the first COVID-19 wave, Spain and Italy experienced the largest effect: an increase in the death rates of 10.59 (10.29–10.88) in Spain and 9.13 (8.96–9.31) in Italy. Following Spain and Italy, a signifcant excess was registered in Sweden, the Netherlands, France, Ireland, Lithuania, Switzerland and Finland. The remaining countries experienced mortality changes that ranged from possible small declines (Germany, Poland, Romania, Denmark, Estonia, Greece, Bulgaria) to non significant increases or decreases (Norway, Portugal, Austria, Czechia, Slovenia, Hungary, Croatia, Luxembourg, Iceland). The heterogeneous geographical effect of the COVID-19 pandemic on mortality can reflect the differences in preparedness of public health system and the policy responses. The effects can be adverse, for instance if the system is not able to handle the increase in hospitalizations from COVID-19 or different diseases, or

Table 4: All-cause excess death in Denmark, Italy, Sweden, and Spain, by sex and age, during three pandemic periods (first covid wave, and first and second epidemic year after the shock). Baseline mortality is obtained with the Modulation Models PS-STFS.

Age	Denmark	Italy	Spain	Sweden
Men				
March to June 2020				
0-64	-119 (-195 ; -45)	1931 (1767 ; 2093)	1188 (986 ; 1387)	284 (230 ; 336)
65-74	-124 (-217 ; -34)	5141 (4854 ; 5424)	3149 (2858 ; 3435)	440 (332 ; 545)
75-84	-55 (-171 ; 57)	9214 (8873 ; 9551)	7265 (6882 ; 7641)	1089 (936 ; 1238)
85	-98 (-162 ; -34)	6823 (6419 ; 7225)	8440 (7978 ; 8896)	1127 (1014 ; 1239)
July 2020 to June 2021				
0-64	-144 (-394 ; 94)	6660 (6203 ; 7112)	2835 (2186 ; 3473)	279 (143 ; 412)
65-74	-315 (-634 ; -12)	14079 (13022 ; 15114)	4305 (3102 ; 5471)	545 (170 ; 904)
75-84	250 (-163 ; 645)	20106 (18987 ; 21212)	8780 (7146 ; 10367)	1140 (562 ; 1695)
85	112 (-55 ; 275)	15182 (13758 ; 16589)	7257 (5179 ; 9279)	702 (365 ; 1032)
July 2021 to June 2022				
0-64	108 (-271 ; 459)	3725 (3148 ; 4294)	2187 (1230 ; 3121)	200 (45 ; 351)
65-74	-19 (-522 ; 447)	5263 (3519 ; 6949)	3314 (1137 ; 5372)	45 (-544 ; 593)
75-84	975 (290 ; 1614)	9970 (8288 ; 11623)	6808 (3825 ; 9639)	926 (-63 ; 1854)
85	772 (574 ; 965)	8573 (6269 ; 10832)	7055 (3056 ; 10855)	520 (58 ; 969)
Women				
March to June 2020				
0-64	-14 (-50 ; 21)	423 (287 ; 557)	822 (687 ; 954)	26 (-16 ; 67)
65-74	-129 (-176 ; -83)	1928 (1698 ; 2153)	1324 (1207 ; 1439)	40 (-47 ; 125)
75-84	4 (-100 ; 104)	5368 (5093 ; 5641)	5656 (5339 ; 5968)	805 (687 ; 920)
85	-301 (-382 ; -222)	14478 (13644 ; 15304)	13658 (13022 ; 14286)	1504 (1298 ; 1705)
July 2020 to June 2021				
0-64	63 (-26 ; 150)	2438 (2042 ; 2828)	816 (397 ; 1226)	-56 (-162 ; 48)
65-74	-191 (-312 ; -74)	6760 (5896 ; 7600)	1727 (1396 ; 2053)	52 (-242 ; 333)
75-84	89 (-272 ; 434)	13651 (12822 ; 14472)	7383 (6089 ; 8638)	1050 (663 ; 1425)
85	-75 (-284 ; 130)	28322 (24138 ; 32409)	6772 (3732 ; 9735)	976 (190 ; 1734)
July 2021 to June 2022				
0-64	191 (93 ; 285)	1390 (868 ; 1902)	981 (385 ; 1561)	5 (-114 ; 121)
65-74	-189 (-328 ; -54)	4043 (2596 ; 5425)	1386 (952 ; 1810)	-97 (-549 ; 322)
75-84	987 (403 ; 1531)	9323 (8170 ; 10459)	6170 (3901 ; 8319)	1275 (684 ; 1838)
85	1007 (759 ; 1250)	27989 (19636 ; 35967)	8966 (2914 ; 14733)	1344 (13 ; 2599)

beneficial, when deaths are avoided because of lockdowns and hygenic measures.

Table 4 reports the excess deaths for men in the original scale of the data, obtained as the difference between the observed and the expected deaths, together with the 95% PI in parentheses. These measures are broken down by age groups and divided by three pandemic phases as described above. No disadvantage was found between sexes in all of the four countries, with the number of excess deaths were similar between men and women. Of the excess deaths that occurred, 48% were in men and 52% were in women

in Denmark, 48% in men and 52% in women in Italy, 53% in men and 47% in women in Spain, and 51% in men and 49% in women in Spain.
Again, mortality rates are better suited for the comparison of sub-groups of the population because they consider its age structure. Mortality rates consider the two forces driving the death rates: the improvements in mortality on one side and the compositional changes on the other side. An increase in the deaths in one age group could be the result of an increase in the number of people in that age group (compositional change) rather than a real change in mortality (mortality improvements).
Figure 7 present the observed death rates (continuous line) and the expected death rates (dashed line) together with the 95% PI (grey shaded area) on the period from March 2020 to June 2022 in Denmark, Italy, Spain, and Sweden, by sex and age groups. The expected death rates and the 95% PI (in the absence of the coronavirus pandemic) are estimated on a common period of the three countries (2010 to February 2020) using the modulation model PS-STFS. The excess mortality outside of the PI is the red shaded area, while the deficit mortality is the blue shaded area. The PI conveniently widen moving away from the starting point of the forecasts, indicating that the uncertainty increases with the forecasting horizon.
Spain and Italy shows a significant excess mortality for both sexes and all age groups during the first COVID-19 wave from March to June 2020. The death rates remained above the levels expected in the winter 2020/2021, and, to a lower extent, during the winter 2021/2022. A summer peak is also visible in 2021. Instead, Danish and Swedish men appear to have experienced several differences over time. Excess mortality in Sweden mainly occurred in 2020 and 2021 and returned to the expected levels in the absence of the pandemic in 2022, whereas in Denmark it mainly took place in 2022.

The differences in the timing of the pandemic impact may reflect the differences in the response policies to the pandemic, with Denmark imposing them in a timely way in 2020 and lifting them in 2022, and Sweden imposing them later on. Denmark and Sweden are very similar in terms of history, social and political systems, they witnessed the spread of COVID-19 around the same time at the beginning of March. Therefore, the differences in the timing of excess death can be attributed to the two radically different responses adopted. The results may also reflect the different vaccination campaigns in the two countries, with Denmark reaching a higher vaccination coverage than Sweden (based on data from the European Centre for Disease Prevention and Control, https://www.ecdc.europa.eu/en/publications-data/data-covid-19-vaccination-eu-eea). In Denmark after the first COVID-19 wave, excess and deficit deaths evened out in the broader age group 0-64, while a deficit of death prevails in the age group 65-74, and an excess in the age group 75-84 and above age 85. In Spain and Sweden, during the whole pandemic period, excess deaths occurred for all the age groups and most of the excess was concentrated in the higher age groups.

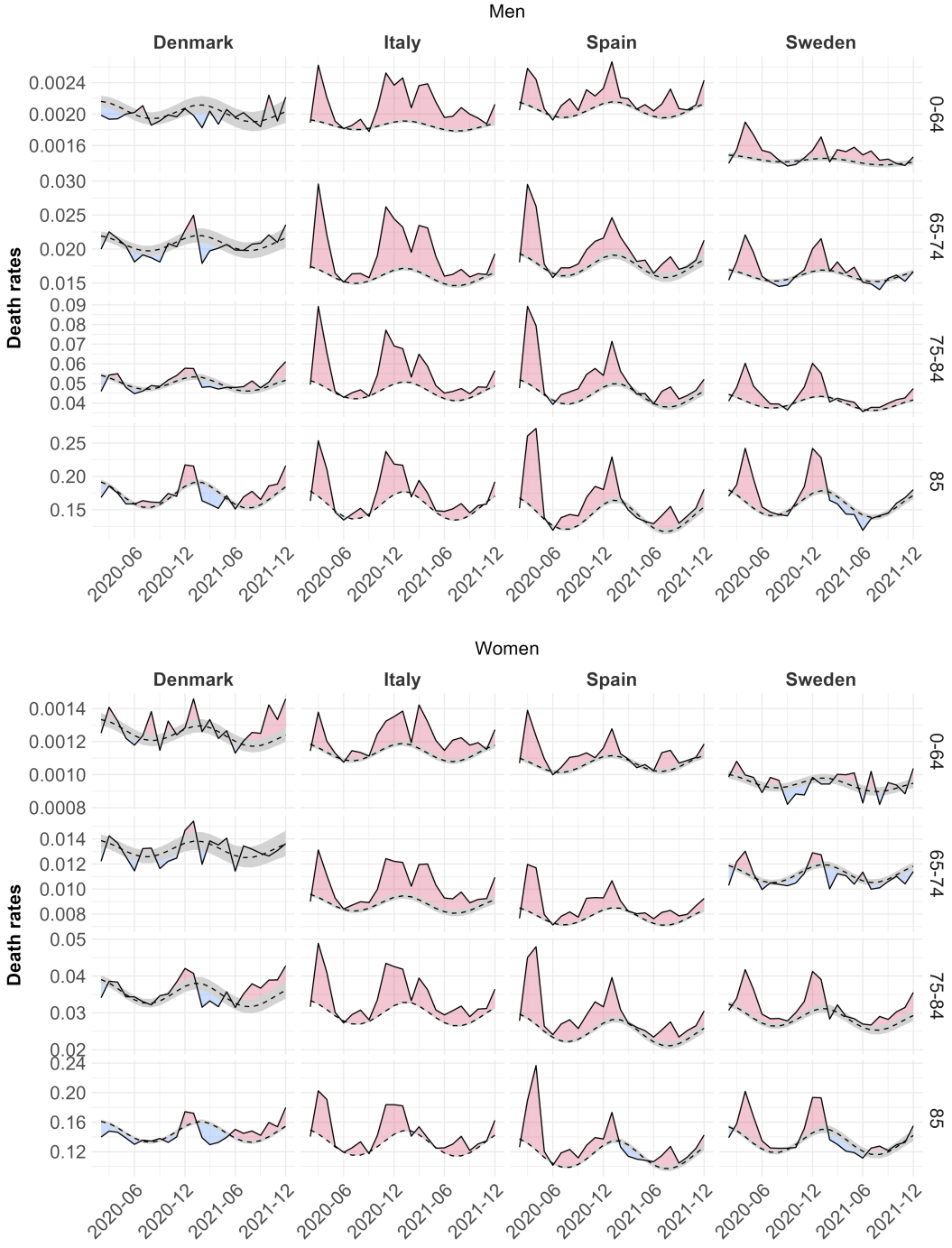

.

Figure 7: **Monthly number of deaths from February 2020 though June 2022 in Denmark, Italy, Sweden, and Spain, by sex and age groups**. The solid line shows the recorded deaths. The dashed line shows the predictions of the expected deaths (obtained with the PS-STFS and PS-STSS models) had the COVID-19 pandemic not occurred. The grey shaded area shows the 95% prediction intervals around the mean prediction. The red shaded area shows the excess deaths and the blue shaded area shows the deficit deaths.

6. Discussion

Before the COVID-19 pandemic, short-term mortality forecasting during an epidemiological year was mainly studied in the domain of epidemiology. After the COVID-19 pandemic, a collective effort to provide data and evidence on the health shock increased interest and the number of publications on excess death from different fields. Numerous estimates of excess mortality have been published using different approaches to forecast the expected mortality without a shock (Kontis et al., 2020; Islam et al., 2021). Among the studies using regression models, many used a Poisson Serfling regression (Serfling, 1963; EuroMOMO, 2017) or more flexible variants of the model assuming smoothed effects (Aburto et al., 2021; Scortichini et al., 2020). However, comparisons of these approaches are lacking. Few studies investigated the sensitivity of excess death estimates, but did not study the accuracy in forecasting the expected deaths on historical periods (Nepomuceno et al., 2022) or did not consider smoothed effects for both the trend and seasonal effects (Schöley, 2021). Our study considers the same family of models and estimation procedure allowing for different degrees of flexibility: the Poisson Serfling model with 1) parametric effect for the trend and seasonality, 2) non-parametric effect for the trend and parametric effect for the seasonality, and 3) non-parametric effect for the trend and seasonality.

For all-cause mortality, the smoothness of the trend appeared to be a desirable feature when forecasting in the short-term. The smoothness of the seasonal component might be a useful assumption in other settings, for instance when the data show a trend of decreasing or increasing seasonal amplitude. Progresses in mortality could lead to a decreasing seasonality which might be better captured with a smooth seasonal component. This could be the case, for instance, of mortality declines in certain historical periods (Ledberg, 2020) or for specific causes of death, such as infectious diseases (Schlüter et al., 2020) or cardiovascular diseases (Crawford et al., 2003).

We illustrated how the PS-STFS model can be used to forecast mortality during the coronavirus pandemic and analyse the vulnerability of a population during the health shock. In order to compare the mortality experiences during the pandemic, one needs to account for the different population sizes and age structures between countries. This can be achieved by considering the exposure in each age group and modelling the mortality rates. All models permit to include the exposures as an offset term and the modulation model showed a competitive forecasting accuracy both for the death counts and for death rates. Therefore, one couls also perform demographic comparisons using modulation models on age-specific death rates or age standardized death rates.

One limitation of the modulation models for forecasting mortality is that the PI of the forecasts increase rather quickly. Therefore, we advise the use of modulation models for one to three years in the future to predict the baseline mortality and to detect excess mortality. One year is usually used to monitor the severity of the influenza season, while two to three years is the time window for pandemics of new infectious diseases to extinguish themself.

Further work on short-term forecasting using modulation models could be to extend the

model to forecast all age groups simultaneously. For instance, a bidimensional model could forecast in the age and year directions simultaneously (Eilers et al., 2008; Currie et al., 2004). Furthermore, modelling the median instead of the mean could better capture the asymmetric shape of the seasonality, because mortality shows a percentage increase during the winter greater than the percentage decrease during the summer.

7. Conclusion

The aim of this paper is to propose a new methodology to model and forecast the baseline mortality that is more flexible compared to the widely used Poisson Serfling model. Specifically, we compare the forecast of the Poisson Serfing model with the modulation model assuming either fixed or smooth seasonal component. The results show that the model with smooth trend and seasonal component (PS-STSS) better fit the historical time series of death counts, followed by the model with smooth trend and fixed seasonal component (PS-STFS). However, the model with smooth trend and fixed seasonal component (PS-STFS) produces more accurate predictions of the expected deaths, indicating that a model with smooth seasonal component may overfit the data. Therefore, accounting for demographic changes by considering smooth trends over longer reference time periods and across age groups is important for reliable estimates of expected deaths. Our short-term mortality predictions come with prediction intervals, whose widths indicate the level of uncertainly associated with the forecast.

8. Acknowledgments

This work was supported by the AXA Research Fund's AXA Chair in Longevity Research (A.-E.L.) and the SCOR Foundation's SCOR Chair on Mortality Research 2023-2026 (S.R.).

References

Aburto, J., Kashyap, R., Schöley, J., Angus, C., Ermisch, J., Mills, M., Dowd, J., 2021. Estimating the burden of the COVID-19 pandemic on mortality, life expectancy and lifespan inequality in England and Wales: a population-level analysis. J Epidemiol Community Health 75, 735–740.

Ansart, S., Pelat, C., Boelle, P.Y., Carrat, F., Flahault, A., Valleron, A.J., 2009. Mortality burden of the 1918–1919 influenza pandemic in Europe. Influenza and other respiratory viruses 3, 99–106.

Basellini, U., Alburez-Gutierrez, D., Del Fava, E., Perrotta, D., Bonetti, M., Camarda, C.G., Zagheni, E., 2021. Linking excess mortality to mobility data during the first wave of covid-19 in England and Wales. SSM-Population Health 14, 100799.

Carballo, A., Durban, M., Kauermann, G., Lee, D., 2019. A general framework for prediction in penalized regression. Statistical Modelling 21, 293–312.

Crawford, V., McCann, M., Stout, R., 2003. Changes in seasonal deaths from myocardial infarction. Qjm 96, 45–52.

Currie, I., Durban, M., Eilers, P., 2004. Smoothing and forecasting mortality rates. Statistical modelling 4, 279–298.

Djeundje, V., Haberman, S., Bajekal, M., Lu, J., 2022. The slowdown in mortality improvement rates 2011–2017: a multi-country analysis. European Actuarial Journal 12, 839–878.

Eilers, P., Gampe, J., Marx, B., Rau, R., 2008. Modulation models for seasonal time series and incidence tables. Statistics in Medicine 27, 3430–3441.

Eilers, P., Marx, B., 1996. Flexible smoothing with B-splines and penalties. Statistical science 11, 89–121.

EuroMOMO, 2017. European monitoring of excess mortality for public health action .

Fouillet, A., Rey, G., Laurent, F., Pavillon, G., Bellec, S., Guihenneuc-Jouyaux, C., Clavel, J., Jougla, E., Hémon, D., 2006. Excess mortality related to the August 2003 heat wave in France. International archives of occupational and environmental health 80, 16–24.

Hastie, T., Tibshirani, R., 1990. Generalized Additive Models .

Hastie, T., Tibshirani, R., 1993. Varying-Coefficient Models. Journal of the Royal Statistical Society Series B: Statistical Methodology 55, 757–779.

Islam, N., Shkolnikov, V., Acosta, R., Klimkin, I., Kawachi, I., Irizarry, R., Alicandro, G., Khunti, K., Yates, T., Jdanov, D., et al., 2021. Excess deaths associated with covid-19 pandemic in 2020: age and sex disaggregated time series analysis in 29 high income countries. bmj 373.

Kontis, V., Bennett, J., Rashid, T., Parks, R., Pearson-Stuttard, J., Guillot, M., Asaria, P., Zhou, B., Battaglini, M., Corsetti, G., et al., 2020. Magnitude, demographics and dynamics of the effect of the first wave of the COVID-19 pandemic on all-cause mortality in 21 industrialized countries. Nature medicine 26, 1919–1928.

Ledberg, A., 2020. A large decrease in the magnitude of seasonal fluctuations in mortality among elderly explains part of the increase in longevity in Sweden during 20th century. BMC Public Health 20, 1–10.

Mazick, A., Gergonne, B., Nielsen, J., Wuillaume, F., Virtanen, M., Fouillet, A., Uphoff, H., Sideroglou, T., Paldy, A., Oza, A., et al., 2012. Excess mortality among the elderly in 12 European countries, February and March 2012. Eurosurveillance 17, 20138.

McCullagh, P., Nelder, J., 1989. Generalized Linear Models. Chapman and Hall.

Missov, T., Patricio, S., Villavicencio, F., 2023. Improvements in age-specific mortality at the oldest ages. arXiv preprint arXiv:2303.16696 .

Mølbak, K., Espenhain, L., Nielsen, J., Tersago, K., Bossuyt, N., Denissov, G., Baburin, A., Virtanen, M., Fouillet, A., Sideroglou, T., et al., 2015. Excess mortality among the elderly in European countries, December 2014 to February 2015. Eurosurveillance 20, 21065.

Németh, L., Jdanov, D.A., Shkolnikov, V.M., 2021. An open-sourced, web-based application to analyze weekly excess mortality based on the Short-term Mortality Fluctuations data series. PLoS One 16, e0246663.

Nepomuceno, M., Klimkin, I., Jdanov, D., Alustiza-Galarza, A., Shkolnikov, V., 2022. Sensitivity analysis of excess mortality due to the COVID-19 pandemic. Population and development review 48, 279–302.

Nielsen, J., Krause, T., Mølbak, K., 2018. Influenza-associated mortality determined from all-cause mortality, Denmark 2010/11-2016/17: the FluMOMO model. Influenza and Other Respiratory Viruses 12, 591–604.

Preston, S., Heuveline, P., Guillot, M., 2001. Demography: Measuring and Modeling Population Processes .

Schlüter, B.S., Masquelier, B., Metcalf, C., Rasoanomenjanahary, A., 2020. Long-term trends in seasonality of mortality in urban Madagascar: the role of the epidemiological transition. Global health action 13, 1717411.

Schöley, J., 2021. Robustness and bias of European excess death estimates in 2020 under varying model specifications. MedRxiv , 2021–06.

Schwarz, G., 1978. Estimating the dimension of a model. The annals of statistics , 461–464.

Scortichini, M., Schneider dos Santos, R., De'Donato, F., De Sario, M., Michelozzi, P., Davoli, M., Masselot, P., Sera, F., Gasparrini, A., 2020. Excess mortality during the COVID-19 outbreak in Italy: a two-stage interrupted time-series analysis. International journal of epidemiology 49, 1909–1917.

Serfling, R., 1963. Methods for current statistical analysis of excess pneumonia-influenza deaths. Public health reports 78, 494.

Stokes, A.C., Lundberg, D.J., Elo, I.T., Hempstead, K., Bor, J., Preston, S.H., 2021. COVID-19 and excess mortality in the United States: A county-level analysis. PLoS medicine 18, e1003571.

Thompson, W., Weintraub, E., Dhankhar, P., Cheng, P.Y., Brammer, L., Meltzer, M., Bresee, J., Shay, D., 2009. Estimates of US influenza-associated deaths made using four different methods. Influenza and other respiratory viruses 3, 37–49.

Toulemon, L., Barbieri, M., 2008. The mortality impact of the August 2003 heat wave in France: investigating the 'harvesting' effect and other long-term consequences. Population studies 62, 39–53.

Appendix A. Model performance

Table A.5 shows the mean BIC values obtained by fitting the three models (PS, PS-STSS and PS-STFS) on the death counts from 2010 to 2019 on a rolling window of 5-years and 10-years. Table 1 The mean BIC favours the model PS-STSS in almost all the countries (21 countries). Either using 5-years or 10-years for the rolling window, the model PS-STSS better fit the series than the PS and the PS-STFS model.

Table A.5: Mean BIC on **death counts** in 25 European countries for multiple fitting periods based on a rolling-window scheme.

	5 years series			10 years series		
	PS	PS-STSS	PS-STFS	PS	PS-STSS	PS-STFS
Austria	1040	994	1021	2047	1996	2019
Bulgaria	1885	1828	1839	3762	3662	3708
Croatia	838	796	817	1641	1605	1635
Czechia	1325	1273	1297	2510	2351	2382
Denmark	650	643	654	1357	1310	1332
Estonia	241	250	251	484	485	487
Finland	598	597	609	1219	1205	1219
France	8158	7492	7941	17074	16109	16605

Germany	10617	9616	10153	21838	20120	20961
Greece	2644	2511	2576	5034	4864	4945
Hungary	2162	2056	2124	4140	4048	4083
Iceland	96	109	109	201	217	216
Ireland	698	691	706	1495	1411	1464
Italy	11279	10048	10592	22338	20633	21466
Lithuania	596	583	592	1452	1235	1246
Luxembourg	109	120	120	219	234	233
Netherlands	1862	1781	1820	3804	3610	3627
Norway	621	595	629	1262	1178	1244
Poland	4861	4488	4687	9811	8967	9451
Portugal	3535	3400	3496	6805	6705	6763
Romania	4165	3778	3881	8973	8142	8614
Slovenia	315	316	323	638	641	650
Spain	9554	8710	9125	19192	18237	18792
Sweden	1100	1074	1101	2225	2214	2234
Switzerland	826	795	826	1634	1613	1628
	4	21	0	4	21	0

Appendix B. Best model based on P-splines

Root mean square error (RMSE) and Mean Absolute Percentage Error (MAPE) of predictions all-cause death counts series for men. A 5-years fitting period is used. Four PS-STSS models are compared: with a first order penalty for both the trend and seasonality (MM-T1S1), with a second order for both the trend and seasonality (MM-T2S2), with a first order for the trend and a second order for the seasonality (MM-T1S2), and with a second order for the trend and first order for the seasonality (MM-T2S1).

Table B.6: Mean RMSE and MAPE on **death counts** in 25 European countries for four combinations of penalties (on trend and seasonality) and for multiple fitting periods based on a rolling-window scheme.

	5 years series								10 years series							
	RMSE				MAPE				RMSE				MAPE			
	t1s1	t2s2	t1s2	t2s1	t1s1	t2s2	t1s2	t2s1	t1s1	t2s2	t1s2	t2s1	t1s1	t2s2	t1s2	t2s1
Austria	381	396	400	375	4	4	4	4	400	377	410	358	4	4	4	4
Bulgaria	591	642	616	619	5	5	5	5	551	574	560	561	5	5	5	5
Croatia	276	312	291	295	5	5	5	5	262	280	274	269	4	5	4	4
Czechia	485	536	530	489	4	4	4	4	467	501	496	469	4	4	4	4
Denmark	240	252	254	235	4	4	4	4	255	239	266	225	5	4	5	4
Estonia	89	84	93	80	5	5	6	4	102	74	105	73	7	4	7	4
Finland	232	240	247	223	4	4	4	4	247	222	255	211	4	4	4	4
France	2812	3163	3111	2906	4	5	5	4	2796	2877	2971	2642	4	4	5	4
Germany	4110	4815	4665	4213	4	5	5	4	4045	4529	4473	4033	4	4	4	4
Greece	681	735	721	688	5	6	6	5	716	697	730	674	5	6	6	5
Hungary	681	747	728	691	5	5	5	5	635	643	662	610	4	4	5	4
Iceland	17	18	18	17	8	9	9	8	19	17	19	16	9	8	9	8
Ireland	179	180	185	177	5	6	6	5	171	160	179	156	5	5	5	5
Italy	3500	4207	3896	3805	5	7	6	6	3421	3878	3655	3633	5	6	5	5
Lithuania	223	226	237	212	5	5	6	5	222	222	225	219	5	5	5	5
Luxembourg	26	29	28	27	7	7	7	7	28	26	28	26	7	6	7	6
Netherlands	678	702	709	670	4	5	5	4	718	682	744	643	4	4	5	4
Norway	207	214	219	203	5	5	5	5	196	197	201	191	5	5	5	5
Poland	1741	1986	1898	1805	4	5	4	4	1766	1862	1876	1724	4	4	4	4
Portugal	734	845	814	773	6	7	6	6	732	756	757	729	6	6	6	6
Romania	1343	1487	1399	1457	5	5	5	5	1254	1333	1308	1287	4	5	5	5
Slovenia	103	111	109	104	5	5	5	5	104	104	108	99	5	5	5	4
Spain	2455	2797	2673	2581	5	6	6	6	2413	2626	2597	2416	5	5	5	5
Sweden	394	424	424	395	4	4	4	4	369	395	395	368	4	4	4	4
Switzerland	298	332	329	302	4	5	5	4	286	286	299	272	4	4	4	4
	16	0	0	9	15	0	0	10	6	0	0	19	7	0	1	17

Table B.7: Mean RMSE and MAPE on **death rates** (x 1000) in 25 European countries for four combinations of penalties (on trend and seasonality) and for multiple fitting periods based on a rolling-window scheme.

	5 years series								10 years series							
	RMSE				MAPE				RMSE				MAPE			
	t1s1	t2s2	t1s2	t2s1	t1s1	t2s2	t1s2	t2s1	t1s1	t2s2	t1s2	t2s1	t1s1	t2s2	t1s2	t2s1
Austria	0.54	0.57	0.57	0.53	4.29	4.50	4.55	4.12	0.54	0.54	0.56	0.51	4.28	4.18	4.44	3.93
Bulgaria	0.97	1.05	1.01	1.01	4.77	5.37	5.02	5.24	1.05	0.98	1.07	0.96	5.10	4.99	5.24	4.80
Croatia	0.79	0.88	0.83	0.83	4.58	5.45	4.86	5.15	0.84	0.82	0.87	0.78	4.56	4.58	4.78	4.41
Czechia	0.55	0.62	0.61	0.56	3.78	4.34	4.26	3.82	0.52	0.56	0.56	0.53	3.60	3.91	3.88	3.63
Denmark	0.55	0.54	0.58	0.51	4.52	4.18	4.79	3.88	0.63	0.51	0.65	0.48	5.63	3.87	5.69	3.64
Estonia	0.75	0.75	0.79	0.72	4.93	4.74	5.22	4.47	0.79	0.67	0.81	0.65	5.46	4.26	5.63	4.13
Finland	0.50	0.54	0.54	0.50	3.89	4.24	4.29	3.90	0.50	0.49	0.52	0.47	3.88	3.85	4.09	3.59
France	0.53	0.59	0.59	0.54	4.40	4.87	5.04	4.46	0.49	0.53	0.54	0.49	4.09	4.57	4.56	4.09
Germany	0.60	0.70	0.69	0.61	4.05	4.80	4.79	4.06	0.60	0.66	0.66	0.59	3.85	4.27	4.44	3.69
Greece	0.75	0.81	0.80	0.76	5.18	5.77	5.57	5.35	0.79	0.77	0.81	0.74	5.44	5.52	5.64	5.26
Hungary	0.80	0.90	0.86	0.83	4.34	5.03	4.81	4.58	0.75	0.78	0.78	0.74	4.04	4.24	4.31	3.95
Iceland	0.64	0.68	0.68	0.65	8.54	8.53	8.87	8.09	0.59	0.61	0.61	0.59	7.66	7.86	8.00	7.59
Ireland	0.57	0.49	0.58	0.48	6.71	5.57	6.90	5.38	0.53	0.42	0.57	0.40	7.07	5.06	7.19	4.86
Italy	0.71	0.86	0.79	0.78	5.25	6.56	6.03	5.88	0.68	0.78	0.73	0.73	4.92	5.73	5.33	5.35
Lithuania	0.89	0.85	0.93	0.82	5.34	5.17	5.59	4.99	0.95	0.88	0.96	0.87	5.61	5.19	5.60	5.21
Luxembourg	0.66	0.68	0.70	0.64	7.47	7.37	7.81	7.03	0.79	0.58	0.80	0.57	9.61	6.43	9.67	6.30
Netherlands	0.49	0.50	0.51	0.48	4.25	4.48	4.59	4.20	0.50	0.49	0.52	0.46	4.39	4.22	4.63	3.90
Norway	0.57	0.53	0.61	0.50	5.53	4.90	5.77	4.68	0.61	0.47	0.62	0.46	6.38	4.51	6.42	4.49
Poland	0.55	0.62	0.60	0.57	3.85	4.52	4.27	4.03	0.56	0.59	0.60	0.54	3.86	4.07	4.21	3.71
Portugal	0.86	0.96	0.94	0.89	5.96	6.91	6.52	6.31	0.87	0.87	0.90	0.84	6.03	6.01	6.11	5.82
Romania	0.77	0.87	0.80	0.85	4.65	5.44	4.81	5.36	0.74	0.79	0.77	0.76	4.36	4.90	4.60	4.68
Slovenia	0.60	0.66	0.64	0.62	4.69	5.18	4.99	4.93	0.61	0.61	0.64	0.58	4.64	4.68	4.93	4.36
Spain	0.66	0.74	0.72	0.69	5.45	6.38	6.12	5.67	0.64	0.67	0.68	0.62	5.30	5.38	5.63	5.00
Sweden	0.54	0.54	0.58	0.51	4.24	4.23	4.60	3.87	0.61	0.49	0.64	0.46	5.52	3.93	5.68	3.52
Switzerland	0.45	0.50	0.50	0.46	4.32	4.68	4.82	4.16	0.45	0.42	0.47	0.40	4.41	3.79	4.63	3.57
	15	0	0	10	12	0	0	13	6	0	0	19	3	1	0	21

Appendix C. Accuracy of the forecasts

Table C.8: Mean RMSE and MAPE on **death counts** in 25 European countries for multiple fitting periods based on a rolling-window scheme.

	5 years series						10 years series					
	RMSE			MAPE			RMSE			MAPE		
	PS	STSS	STFS	PS	STSS	STFS	PS	STSS	STFS	PS	STSS	STFS
Austria	368	375	370	4.06	4.12	4.06	363	358	356	3.98	3.85	3.84
Bulgaria	600	619	616	4.97	5.19	5.15	570	561	567	4.73	4.73	4.72
Croatia	285	295	289	4.98	5.20	5.10	269	269	266	4.35	4.37	4.39
Czechia	486	489	478	3.87	3.85	3.70	467	469	461	3.74	3.70	3.62
Denmark	233	235	231	3.88	3.90	3.86	227	225	219	3.82	3.65	3.59
Estonia	79	80	80	4.34	4.43	4.42	77	73	73	4.34	4.15	4.10
Finland	220	223	223	3.84	3.89	3.94	215	211	210	3.66	3.62	3.60
France	2757	2906	2855	4.11	4.43	4.35	2531	2642	2537	3.75	4.00	3.78
Germany	4050	4213	4090	3.88	4.09	3.97	3962	4033	3926	3.65	3.67	3.57
Greece	689	688	681	5.36	5.35	5.28	660	674	678	5.08	5.26	5.24
Hungary	662	691	680	4.29	4.58	4.46	606	610	612	3.80	3.94	3.94
Iceland	17	17	17	8.10	8.12	8.12	16	16	16	7.63	7.71	7.71
Ireland	178	177	179	5.33	5.35	5.47	164	156	156	4.99	4.76	4.81
Italy	3500	3805	3767	5.33	5.84	5.79	3389	3633	3574	4.99	5.36	5.27
Lithuania	216	212	207	5.08	4.94	4.81	259	219	219	6.20	5.15	5.16
Luxembourg	27	27	27	6.85	7.03	7.03	26	26	26	6.28	6.34	6.37
Netherlands	651	670	667	4.02	4.22	4.19	696	643	636	4.40	3.91	3.89
Norway	210	203	209	4.83	4.66	4.80	211	191	207	5.06	4.52	5.00
Poland	1698	1805	1771	3.79	4.06	4.04	1780	1724	1705	4.00	3.71	3.72
Portugal	731	773	771	5.81	6.32	6.36	708	729	721	5.58	5.86	5.80
Romania	1396	1457	1458	5.06	5.30	5.30	1244	1287	1304	4.27	4.68	4.68
Slovenia	102	104	104	4.88	4.91	4.92	99	99	99	4.36	4.36	4.32
Spain	2447	2581	2525	5.42	5.70	5.52	2339	2416	2358	4.93	5.01	4.90
Sweden	398	395	391	3.85	3.86	3.80	364	368	365	3.46	3.53	3.52
Switzerland	293	302	297	4.06	4.24	4.16	273	272	269	3.73	3.63	3.57
	17	3	5	19	0	6	8	6	11	10	4	11

Appendix D. Excess death during the COVID-19 pandemic

Table D.9: All-cause excess death rates (x 1000) in Europe during three pandemic periods (first covid wave, and first and second epidemic year after the shock). Baseline mortality is obtained with the Modulation Models PS-STFS.

country	March to June 2020	July 2020 to June 2021	July 2021 to June 2022
Austria	-0.19 (-0.8 ; 0.41)	11.8 (9.17 ; 14.37)	7.34 (5.28 ; 9.33)
Bulgaria	-3.76 (-4.29 ; -3.23)	61.45 (59.88 ; 63.01)	45.59 (44.64 ; 46.53)
Croatia	-0.99 (-2.03 ; 0.04)	35.84 (31.49 ; 40.07)	25.67 (22.35 ; 28.85)
Czechia	-0.56 (-1.21 ; 0.08)	42.04 (38.98 ; 45.02)	9.96 (7.47 ; 12.36)
Denmark	-0.96 (-1.7 ; -0.24)	2.2 (-0.9 ; 5.2)	6.97 (4.59 ; 9.25)
Estonia	-0.97 (-1.8 ; -0.15)	16.61 (14.42 ; 18.75)	14.12 (12.93 ; 15.29)
Finland	0.52 (0.11 ; 0.94)	1.15 (-0.02 ; 2.31)	6.74 (6.05 ; 7.42)
France	2.92 (2.76 ; 3.07)	9.36 (8.84 ; 9.87)	3.41 (3.06 ; 3.76)
Germany	-0.34 (-0.58 ; -0.11)	10.2 (9.11 ; 11.28)	8.45 (7.59 ; 9.31)
Greece	-3.36 (-4.07 ; -2.65)	4.97 (1.49 ; 8.37)	11.86 (8.96 ; 14.66)
Hungary	-0.62 (-1.33 ; 0.08)	42.17 (39.07 ; 45.21)	20.19 (17.78 ; 22.53)
Iceland	-1.22 (-2.58 ; 0.08)	-2.25 (-6.12 ; 1.44)	-0.35 (-2.67 ; 1.83)
Ireland	2.39 (1.88 ; 2.89)	2.14 (0.36 ; 3.87)	3.33 (2.1 ; 4.51)
Italy	9.13 (8.96 ; 9.31)	22.28 (21.69 ; 22.87)	7.39 (7.01 ; 7.78)
Lithuania	2.11 (1.13 ; 3.07)	41.56 (38.26 ; 44.8)	28.14 (25.91 ; 30.3)
Luxembourg	-1.03 (-2.09 ; 0)	5.46 (2.5 ; 8.31)	1.94 (0.22 ; 3.59)
Netherlands	4.83 (4.44 ; 5.22)	8.59 (7.03 ; 10.13)	8.39 (7.22 ; 9.54)
Norway	0.66 (-0.19 ; 1.48)	1.01 (-1.88 ; 3.81)	1.55 (-0.47 ; 3.48)
Poland	-0.58 (-0.82 ; -0.34)	41.48 (40.73 ; 42.22)	16.25 (15.77 ; 16.72)
Portugal	0.08 (-0.27 ; 0.43)	16.96 (15.93 ; 17.99)	2.97 (2.35 ; 3.58)
Romania	-0.86 (-1.26 ; -0.47)	42.05 (40.61 ; 43.47)	33.38 (32.37 ; 34.37)
Slovenia	-0.59 (-1.66 ; 0.45)	24.23 (20.27 ; 28.06)	8.75 (5.91 ; 11.45)
Spain	10.59 (10.29 ; 10.88)	10.26 (8.8 ; 11.7)	5.03 (3.84 ; 6.19)
Sweden	6.55 (5.98 ; 7.1)	6.45 (3.92 ; 8.93)	3.1 (1.08 ; 5.04)
Switzerland	0.86 (0.34 ; 1.37)	10.62 (8.53 ; 12.66)	4.14 (2.55 ; 5.67)

Table D.10: All-cause excess death in Denmark, Italy, Sweden, and Spain, by sex and age, during three pandemic periods (first covid wave, and first and second epidemic year after the shock). Baseline mortality is obtained with the Modulation Models PS-STFS.

Age	Denmark	Italy	Spain	Sweden
Men				
March to June 2020				
0-64	-0.6 (-0.9 ; -0.2)	1.1 (1 ; 1.2)	0.7 (0.6 ; 0.8)	0.8 (0.7 ; 1)
65-74	-2.8 (-6.3 ; 0.6)	18.5 (17.6 ; 19.5)	17.8 (16.2 ; 19.3)	9.8 (8.4 ; 11.3)
75-84	-7.4 (-13.4 ; -1.5)	56.1 (54.1 ; 58)	65.5 (62 ; 68.9)	36 (33 ; 39)
85	-34.2 (-51.7 ; -17.1)	112.7 (107.2 ; 118.1)	205.3 (195.2 ; 215.3)	139.2 (123.9 ; 154.2)
July 2020 to June 2021				
0-64	-0.6 (-1.9 ; 0.5)	3.7 (3.4 ; 3.9)	1.9 (1.6 ; 2.1)	0.9 (0.5 ; 1.3)
65-74	-7 (-18.8 ; 4.2)	51 (47.6 ; 54.3)	24.4 (18.1 ; 30.5)	9.7 (5.9 ; 13.4)
75-84	4.9 (-13 ; 22.3)	120.4 (113.8 ; 126.9)	78.7 (64.2 ; 92.7)	40.4 (32.6 ; 48.1)
85	-2 (-46.5 ; 41.5)	253.5 (237 ; 269.8)	210.1 (166.2 ; 252.9)	69.8 (22.3 ; 116.2)
July 2021 to June 2022				
0-64	0.5 (-0.3 ; 1.2)	1.1 (0.9 ; 1.2)	1 (0.8 ; 1.1)	0.3 (0.1 ; 0.5)
65-74	5.2 (-2.9 ; 12.8)	8.8 (6.5 ; 11.1)	9.6 (4.9 ; 14.2)	-1.8 (-3.9 ; 0.2)
75-84	26.2 (15.2 ; 36.8)	25.4 (21 ; 29.7)	32.7 (21.9 ; 43.1)	16.3 (12.1 ; 20.5)
85	113.7 (90.2 ; 136.6)	68.4 (58.3 ; 78.5)	110.6 (77.1 ; 142.7)	18.3 (-11.7 ; 47.3)
Women				
March to June 2020				
0-64	-0.1 (-0.3 ; 0.1)	0.2 (0.2 ; 0.3)	0.5 (0.4 ; 0.6)	0.1 (0 ; 0.2)
65-74	-2.5 (-5 ; 0)	6 (5.3 ; 6.7)	6.9 (6.4 ; 7.4)	0.3 (-0.9 ; 1.5)
75-84	-2.6 (-8.2 ; 3)	25.2 (24.1 ; 26.3)	37.7 (35.5 ; 39.8)	22.8 (19.1 ; 26.4)
85	-52.3 (-64.2 ; -40.6)	105.7 (102.2 ; 109.2)	166.3 (159.2 ; 173.3)	103.4 (89.1 ; 117.5)
July 2020 to June 2021				
0-64	0.3 (-0.1 ; 0.8)	1.4 (1.2 ; 1.5)	0.5 (0.3 ; 0.7)	-0.1 (-0.4 ; 0.2)
65-74	-0.4 (-8.7 ; 7.5)	21.6 (19 ; 24.1)	9.7 (8.3 ; 11.2)	-2.1 (-5.2 ; 0.9)
75-84	-1.3 (-20.4 ; 16.9)	62.1 (59.1 ; 65.1)	48.2 (39.5 ; 56.5)	30.6 (18.3 ; 42.4)
85	-40.7 (-71.4 ; -10.6)	177.2 (166.8 ; 187.5)	105.9 (73.1 ; 138)	49.8 (-4.4 ; 102.2)
July 2021 to June 2022				
0-64	0.7 (0.5 ; 1)	0.5 (0.4 ; 0.6)	0.3 (0.2 ; 0.4)	0.1 (0 ; 0.3)
65-74	1.2 (-4.4 ; 6.4)	6.2 (4.4 ; 7.9)	4.6 (3.7 ; 5.4)	-2.8 (-4.5 ; -1.2)
75-84	30.1 (17.4 ; 42.1)	19.9 (18.1 ; 21.6)	21.6 (15.3 ; 27.6)	20.4 (12.3 ; 28.1)
85	84.3 (67.9 ; 100.5)	70.9 (64.5 ; 77.2)	78.9 (53.2 ; 103.6)	36.1 (-2.6 ; 72.8)